ADVANCED FUNCTIONAL MATERIALS
www.afm-journal.de

Healable, Stable and Stiff Hydrogels: Combining Conflicting Properties Using Dynamic and Selective Three-Component Recognition with Reinforcing Cellulose Nanorods

Jason R. McKee, Eric A. Appel, Jani Seitsonen, Eero Kontturi, Oren A. Scherman, and Olli Ikkala**

Nanocomposite hydrogels are prepared combining polymer brush-modified 'hard' cellulose nanocrystals (CNC) and 'soft' polymeric domains, and bound together by cucurbit[8]uril (CB[8]) supramolecular crosslinks, which allow dynamic host–guest interactions as well as selective and simultaneous binding of two guests, i.e., methyl viologen (the first guest) and naphthyl units (the second guest). CNCs are mechanically strong colloidal rods with nanometer-scale lateral dimensions, which are functionalized by surface-initiated atom transfer radical polymerization to yield a dense set of methacrylate polymer brushes bearing naphthyl units. They can then be non-covalently cross-linked through simple addition of poly(vinyl alcohol) polymers containing pendant viologen units as well as CB[8]s in aqueous media. The resulting supramolecular nanocomposite hydrogels combine three important criteria: high storage modulus ($G' > 10$ kPa), rapid sol–gel transition (<6 s), and rapid self-healing even upon aging for several months, as driven by balanced colloidal reinforcement as well as the selectivity and dynamics of the CB[8] three-component supramolecular interactions. Such a new combination of properties for stiff and self-healing hydrogel materials suggests new approaches for advanced dynamic materials from renewable sources.

1. Introduction

In materials science, one of the grand challenges is to combine conflicting and seemingly mutually exclusive properties within a single material to achieve multiple functionalities. One broad challenge is to combine high stiffness with properties requiring high molecular dynamics. Herein, we aim at a concept for high modulus nanocomposite supramolecular hydrogels, which demonstrate rapid re-formation of the aqueous networks following processing in the fluid sol-state, as well as rapid and temporally stable healing of the network after mechanical break without passivating side-reactions upon aging. Even though a plethora of supramolecular hydrogels have been presented, this combination of properties is highly uncommon yet desirable in such materials.[1–16] Rapid re-formation of the gel-state from the sol-state suggests incorporating highly dynamic supramolecular cross-links to form the networks. However, combining high mechanical stiffness with dynamic cross-links may seem a conflicting and opposite requirement as high hydrogel stiffness at first sight suggests strong and stable cross-linking interactions.[17] Long-term stability for the healing capability upon aging, on the other hand, would suggest incorporation of highly specific supramolecular interactions in order to suppress unwanted side-interactions, especially passivation of the exposed surface areas, which generally would impede the temporal stability. Supramolecular hydrogels have been reported combining one or two of these conflicting properties.[1–16] For example, self-healing of mechanically stiff supramolecular hydrogels based on negatively charged nanoclay sheets bound together electrostatically with positively charged dendritic 'molecular binders' has been reported.[1] Therein, when the cut pieces were pressed together, they exhibited rapid sol-to-gel recovery within minutes. However, the observed self-healing quickly became passivated over time, as the exposed ionic interactions were not specific, thus being prone to unwanted side reactions. On the other hand, mechanically strong hydrogels exhibiting self-healing after prolonged aging have been prepared using nanoclays bearing physically interacting polymer brushes by rearrangement of their entanglements.[7] However, the timescale for self-healing was long on account of slow polymer dynamics.

J. R. McKee, Dr. J. Seitsonen, Prof. O. Ikkala
Molecular Materials, Department of Applied Physics
Aalto University (previously Helsinki University of Technology)
P.O. Box 15100, FIN-00076, Espoo, Finland
E-mail: Olli.Ikkala@aalto.fi
Dr. E. A. Appel, Dr. O. A. Scherman
Melville Laboratory for Polymer Synthesis
Department of Chemistry
University of Cambridge
Lensfield Road, Cambridge CB21EW, UK
E-mail: oas23@cam.ac.uk
Dr. E. Kontturi
Department of Forest Products Technology
Aalto University
P.O. Box 16300, FIN-00076, Aalto, Espoo, Finland

DOI: 10.1002/adfm.201303699

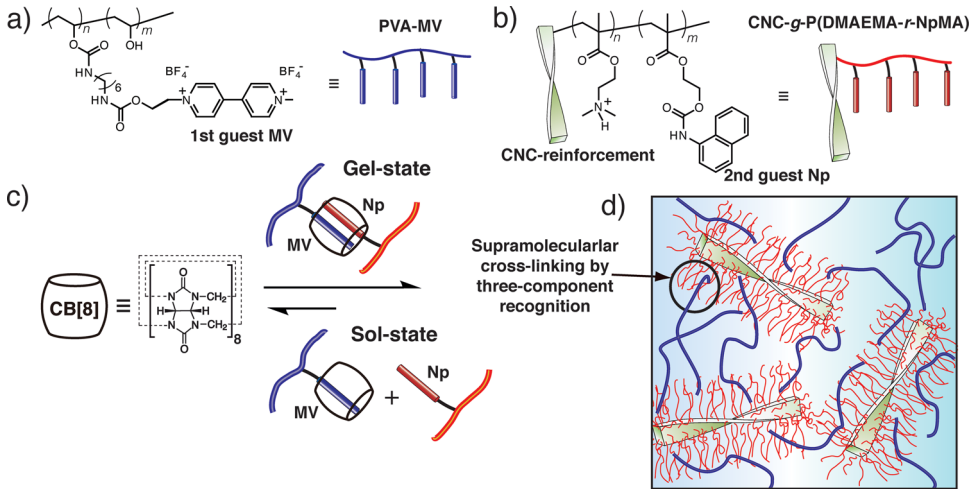

Figure 1. Schematics and architecture for highly specific, dynamic and stiff three-component recognition-driven supramolecular hydrogels based on cellulose nanocrystals (CNC) and CB[8] host-guest chemistry. a) Poly(vinyl alcohol) (PVA) containing the first-guest methyl viologen functionality (PVA-MV). b) CNCs containing copolymer grafts of protonated dimethylaminoethyl methacrylate (DMAEMA) and second-guest naphthyl methacrylate (NpMA) repeat units (CNC-*g*-P(DMAEMA-*r*-NpMA)) with DMAEMA/NpMA ~ 10/1 mol/mol. c) CB[8] as the host motif. d) Selective supramolecular cross-links based on three-component recognition by CB[8] binding together the components into dynamic hydrogels where the modified PVA bridges the CNC-grafts together. The chiral twist of CNC is also schematically shown.

Hence, the combination of rapid network healing and robust sol-gel recovery with suppressed passivation as well as promoted mechanical properties requires new concepts for supramolecular hydrogels. We approached these conflicting requirements by combining two hypotheses. The first hypothesis was that highly selective yet still dynamic supramolecular host-guest interactions could suppress unwanted side-interactions in self-healing, unlike those observed for bare ionic interactions and hydrogen bonds. For example, cyclodextrins are cyclic oligosaccharides which have been shown to selectively bind with specific guest motifs.[2–6,15,18] Recently, two-component host-guest interactions based on cyclodextrins and tailored guests have lead to hydrogels with selective recognition and stimulus-responsive healing by tuning the host-guest interactions.[2–6,15] For promoted selectivity, we selected the three-component host-guest interactions of cucurbit[8]uril (CB[8]), which it is a macrocyclic molecule with a large internal diameter of 8.8 Å.[19–21] It exhibits high equilibrium binding constants (K_{eq} up to 10^{12} M^{-2}) while maintaining selectivity for two guests, which in combination leads to a high rate of guest exchange.[13,14,22,23] The second hypothesis was to use particularly strong reinforcing nanoscale elements to enhance the hydrogel modulus bound within a soft physically cross-linked material. Native rod-like cellulose nanocrystals (CNCs) are particularly interesting on account of their wide availability from sustainable resources and as they can be used for composites and functional materials.[24–31] CNCs have lateral dimensions in the range of a few nanometers with lengths ranging between 100–300 nm. The native crystalline cellulose structure within CNCs involves parallel grossly hydrogen bonded cellulose chains and such a structure leads to excellent mechanical properties with modulus values up to ca. 140 GPa and strength in the range of several GPa, even approaching those of, for example, steel.[32,33] Recently, controlled polymerization techniques have been shown to allow well defined polymer brushes on the CNC nanorods to control the surface activity, compatibility, and interactions to other structural components.[34–38]

To combine these hypothesis, we designed a three component hydrogel architecture (**Figure 1**) that contained: reinforcing CNC-colloidal rods decorated with second-guest functional polymer brushes; linear first-guest functional polymers to bridge the CNCs together; and CB[8] to physically bind everything together. The gelation was studied as a function of composition, the sol–gel transitions were studied using dynamic rheology and the healing with suppressed passivation was demonstrated.

2. Results and Discussion

2.1. Synthesis of the CB[8] Guest Functional Constituents

To embed the 'hard' reinforcing CNCs into the soft CB[8] bound hydrogel, we attached random copolymer grafts consisting of dimethylaminoethyl methacrylate (DMAEMA) and second guest napthyl-functionalized methacrylate (NpMA) repeating units to the CNC surface; denoted as CNC-*g*-P(DMAEMA-*r*-NpMA) (Figure 1b). Our initial hypothesis was that by covalently attaching functionalized polymer brushes onto CNCs, more efficient stress-transfer would be obtained as well as a more homogeneous dispersion of CNCs throughout the physical network. In order to facilitate surface-initiated atom transfer radical polymerization (SI-ATRP) of the polymer brushes on the CNCs, the latter surfaces were first brominated in two steps to allow initiation of the polymerization; first by gas phase chemical vapour deposition of freeze-dried open porous CNC aerogels using α-bromoisobutyryl bromide (BriBBr), followed by liquid phase reactions using BriBBr

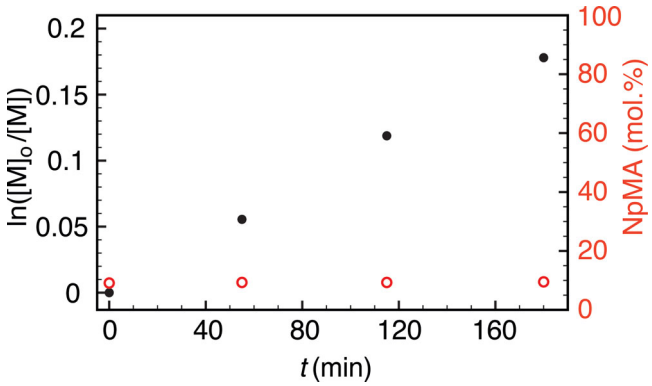

Figure 2. Kinetic data obtained from the surface initiated atom transfer radical polymerization (SI-ATRP) of dimethylaminoethyl methacrylate (DMAEMA) and 2-naphthylurethane ethyl methacrylate (NpMA) monomers onto CNC surface: semilogarithmic plot derived from the evolution of conversion as a function of time (solid), as determined by ^{1}H NMR recorded in $CDCl_3$; relative molar ratio of the unreacted NpMA moieties to the unreacted DMAEMA (hollow), as determined by 1H NMR ($CDCl_3$). The conversions were determined by comparing the disappearing vinyl signals (5.5 and 6.0 ppm) to the emerging polymer pendant methyl signal (0.7–1.1 ppm), characteristic to methacrylic polymers. The reaction was quenched at the 16.3% conversion. The change in the monomer ratios between DMAEMA and NpMA was followed by ^{1}H NMR throughout the polymerisation by comparing the DMAEMA and NpMA vinyl signal integrals (6.04, 5.50 ppm and 6.09, 5.53 ppm respectively). Accordingly, the mean loading of NpMA within the polymer brushes was calculated as 9.5 mol.% for the final product.

to further promote the level of the bromination, as described previously[38] (the detailed synthetic route is described in the SI). The random copolymer grafts attached to the CNCs were polymerized via SI-ATRP with an initial monomer molar ratio of [DMAEMA]/[NpMA] = [10]/[1] (Scheme S1). This ratio of Np-units along the polymeric backbone has been previously shown to work well for hydrogels networks involving two 'soft' polymeric components forming the hydrogel networks.[13,14] The SI-ATRP was catalyzed by a Cu(I)/hexamethyltriethylenetetramine ligand complex. Dimethylformamide (DMF) was chosen as a solvent as it formed a strong polar solvent media that yielded a good dispersion of initiator modified CNCs (CNC-Br).[38] This polymerization was done with a high amount of monomer over initiator [M]/ [I] ~ [2200]/[1] aiming at longer brushes at lower conversions. This was important as the conversion had to be limited to prevent unwanted termination and chain-transfer reactions.

During the surface-initiated polymerization of the second-guest functional graft, kinetic samples were taken at 60 min time intervals to determine the evolution of conversion as well as the monomer composition of the graft. Here, the conversions were determined by comparing the disappearing vinyl signals (5.5 and 6.0 ppm) to the emerging polymer pendant methyl signal (0.7–1.1 ppm). This reaction demonstrated linear evolution of conversion as a function of time (**Figure 2**). The reaction was stopped at 16.3% conversion to minimize any possibility of termination by combination. According to the final conversion, the graft copolymer had a number average molecular weight of ca. 88 ± 5 kg mol^{-1}, as determined by ^{1}H NMR when taking into account initiator efficiency of approximately 69%, determined previously for these CNC-Br initiators under similar polymerization conditions.[38] Moreover, the change in the monomer ratios between DMAEMA and NpMA was followed by ^{1}H NMR. Here, the vinyl signals for DMAEMA and Np-MA integrals, 6.04, 5.50 ppm and 6.09, 5.53 ppm respectively, were compared to each other at each time interval to determine a possible gradient difference in the system (Figure 2). However, due to the similar chemical nature of the monomers, little difference in the gradient was observed – with a relative molar amount of Np-MA being 9.1 mol.% at start of the reaction and 9.5 mol.% at 16.3% conversion. It could, therefore, be concluded that Np-MA had homogeneously polymerized alongside DMAEMA throughout the graft. A ^{1}H NMR spectrum of the final purified product CNC-*g*-P(DMAEMA-*r*-NpMA) is shown in Figure S1 as well as qualitative characterization by FT-IR (Figure S2).

The complementary 'soft' poly(vinyl alcohol) (PVA) chains with a molecular weight M_n = 200 kg mol^{-1} and pendant methyl viologen (MV) functionalities (5 mol.% loading), denoted as PVA-MV (Figure 1a) were synthesized according to previous literature procedures.[14]

2.2. Forming the Supramolecular Nanocomposite Hydrogel

Herein, we prepared three-component nanocomposite hydrogels (Figure 1) consisting of: 1) The supramolecular host CB[8] to simultaneously bind methyl viologen- and naphthyl-based units as the first and second guests, respectively (Figure 1c);[39] 2) 'Hard' reinforcing colloidal rod-like CNCs with attached random copolymer grafts (CNC-*g*-P(DMAEMA-*r*-NpMA)) functionalized with second-guest naphtyl functionality (9.5 mol.% loading) (Figure 1b); 3) 'Soft' PVA chains containing pendant first-guest methyl viologen functionalities (5 mol.% loading) (Figure 1a).[14] The ensuing nanocomposite hydrogels were formed by combining an acidic (pH = 0.5) dispersion of CNC-*g*-P(DMAEMA-*r*-NpMA) with an aqueous solution containing both PVA-MV and CB[8] (**Table 1**). The low pH was found to greatly increase the colloidal stability of the CNC-*g*-P(DMAEMA-*r*-NpMA) as well as to facilitate the gel formation, due to increased electrostatic repulsion within the grafts. We expected the optimal composition to be close to the equimolar amount of viologen and naphthyl units with a slight excess of CB[8] units to provide a facile host availability (see also later **Figure 3**). Therefore we selected a fixed ratio mol CB[8]/mol MV = 1.2/1.0 mol/mol which was obtained by using the concentrations of PVA-MV (10 mg/mL) and CB[8] (10 mg/mL), see Table 1. To find the optimal aqueous composition for the relative molar amount of the naphthyl units versus methyl viologens, their ratio was systematically increased from 0.54 to 1.65, i.e. past the nominal stoichiometric value 1.0, by adding increased concentration of CNC-*g*-P(DMAEMA-*r*-NpMA) from 10 to 30 mg/mL (Table 1). By combining the two solutions, a reddish aqueous precipitate formed, which quickly fused together under centrifugation (5000 rpm for 10 min) to form a homogeneous aqueous rubbery material that was in stable equilibrium with the surrounding water (**Figure 4**).

Table 1. The studied aqueous compositions of CNC-*g*-P(DMAEMA-*r*-NpMA)/PVA-MV/CB[8] by adding Aqueous dispersion component 1 containing CNC-*g*-P(DMAEMA-*r*-NpMA) and Aqueous solution component 2 containing PVA-MV and CB[8]. The latter solution involved a slight 20% molar excess of CB[8] vs MV to promote accessibility of the CB[8] units. By adding different amounts of CNC-*g*-P(DMAEMA-*r*-NpMA), the relative molar amounts of Np and MV could be tuned across their stoichiometric value 1. The table shows the relative molar ratios of Np over MV: solution volume and concentrations for each component; solids content, as determined right after the rheological measurements; zero-strain complex viscosity and storage modulus (*G′*), as determined via strain amplitude dependant oscillatory measurements at 0.1–1.0% strain. Not surprisingly, the composition at the 3rd entry (relation Np:MV 1.1 mol), i.e. close to the stoichiometric relation, renders the highest storage modulus *G′* and was discussed more detail. Note that the entry 3 shows close to stoichiometric composition, allowing the highest modulus.

	Aqueous component 1 [1 mL]	Aqueous component 2 [1 mL]					
Np/MV [mol/mol]	CNC-*g*-P(DMAEMA-*r*-NpMA) [mg/mL]	PVA-MV [mg/mL]	CB[8] [mg/mL]	CB[8]/MV [mol/mol]	Solids Cont. [%]	Complex Viscosity [Pa s]	*G′* [Pa]
0.54	10	10	10	1.2	11.4	390	3800
0.83	15	10	10	1.2	14.4	980	9400
1.1	20	10	10	1.2	18.6	1490	14300
1.4	25	10	10	1.2	15.7	820	7900
1.65	30	10	10	1.2	9	620	6000

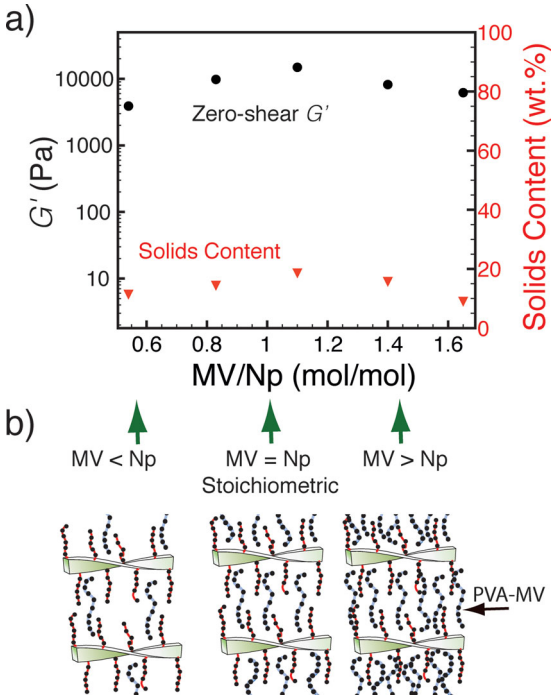

Figure 3. a) Zero-shear *G'* values for NC-*g*-P(DMAEMA-*r*-NpMA)/PVA-MV/CB[8]-based hydrogels. The relative molar amount of methyl viologen *vs.* naphthyl units was tuned past the nominal stoichiometric value 1.0 by increasing the CNC-*g*-P(DMAEMA-*r*-NpMA) content by keeping a fixed ratio mol CB[8] / mol MV = 1.2/1.0 mol/mol, i.e., a slight molar excess of CB[8] vs MV. The maximum *G´* is observed for the close to stoichiometric molar composition Np/MV 1.1 mol (Table 1: entry 3). The corresponding solids content for each sample is determined directly following the rheological measurements. b) The schematic effect of the PVA-MV-mediated bridging based, as tuned by the Np/MV ratio, with less efficient bridging with non-stoichiometric guest ratios, and the nominally stoichiometric Np/MV ratio where the system demonstrates the highest *G'* and solids content. For clarity, the CB[8]´s have not been plotted, the dots mark the MP and MV sites.

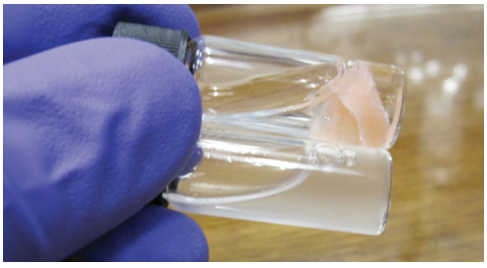

Figure 4. The formed CNC-*g*-P(DMAEMA-*r*-NpMA)/PVA-MV/CB[8]-based hydrogel (top sample, for composition, see Table 1, entry 1) and the control sample (bottom sample) that contained the first and second guest functional components (CNC-*g*-P(DMAEMA-*r*-NpMA) and PVA-MV) at similar composition without CB[8] – note the absence of red colour and any precipitate formation. Also, note the change in volume and the clear supernatant in the top sample due to centrifugation step.

2.3. Characterization of the Selective Ternary Binding

The host-guest binding of the components was investigated by isothermal titration calorimetry (ITC), which suggested that almost all of the guest components, even the Np-motifs deep within the cationic P(DMAEMA-*r*-NpMA)-grafts played a part in the ternary complexation process (Figure S3). Indirectly, this also means that selecting non-stoichiometric molar ratios between the Np and MV motifs would lead to less optimal 'bridging' between the CNC-grafts. In this context, the major driving force for the promoted mechanical properties arose from the stoichiometric Np/MV-guest ratios, which lead to stronger bridging between the reinforcing CNC-grafts, higher solids contents, and a more efficient stress-transfer from the soft dynamically cross-linked PVA/PDMAEMA domains to the hard CNC domains (Figure 3, Table 1). This is in conceptual contrast to more classical nanocomposite systems where higher concentrations of the hard reinforcing components typically lead to higher storage moduli.

2.4. Mechanical Properties of the Dynamic Network

Dynamic oscillatory rheometry showed the highest zero-stress storage modulus G' = 14.3 kPa for the composition with a close stoichiometric relation between the Np and MV groups, as expected (Figure 3, Figure S4 and Figure S5; Table 1: entry 3). This composition had a total solids content of 18.6 wt.%. The main emphasis is subsequently in this composition (for the other compositions, see SI). The present G' is a high value in comparison to most supramolecular hydrogels, which typically demonstrate G'-values below 1 kPa.[40–43] In rare cases, higher values are observed for supramolecular hydrogels;[1] however, they tend to show lower sol-gel rates and time-dependent passivation in their self-healing capacity. We would like to emphasize that increasing the stiffness of gel-networks bound together purely by supramolecular interactions while retaining high dynamics is non-trivial. For example, previous CB[8]-bound networks are limited by the solubility limit for the CB[8] motif, which has limited the maximum loading of polymeric constituents, and thus the ensuing modulus values to ca. 1 kPa.[13] Hence, to circumvent these issues, new architectures are required as shown herein.

All three components CNC-*g*-P(DMAEMA-*r*-NpMA), PVA-MV, and CB[8] are required for the gel formation. The polymer-brush modified colloidal CNC-*g*-P(DMAEMA-*r*-NpMA) rods alone remained as free-flowing electrostatically stabilized aqueous liquids, even at high concentrations (5 wt%). Again, this is in stark contrast to previous work,[1] where the reinforcing nanoclay sheets formed gels on their own and the added dendritic 'molecular binder' serves primarily to bolster the gel modulus. Further, mixing CNC-*g*-P(DMAEMA-*r*-NpMA) and PVA-MV without any CB[8] did not result in observable increase in solution viscosity, colour change, or hydrogel formation (Figure 4). The interplay of the binding selectivity and kinetics of the CB[8] and the reinforcing ability of the CNCs is a key issue in the presented gels. Thus, our hydrogels underwent a complete transition from viscous fluid to the gel state (sol-to-gel) exclusively on account of CB[8] ternary complex formation. Moreover, even the low pH (pH = 0.5) of the constituent solutions demonstrated the robust nature of the CB[8]-based cross-linking, whereby even high ionic strength had little or no effect on the supramolecular binding process.

Frequency dependent oscillatory rheology indicated that the storage modulus (G') was almost constant *vs.* frequency and the storage modulus was much larger than the loss modulus $G' >> G''$ (**Figure 5**a and Figure S7), which are indicators of gelation.[44,45] There was a slight increase in both G' and G'' as a function of increasing frequency, regardless of the material composition, which is in accordance with previous observations of other CB[8]-based hydrogels.[13,14] However, these previous gels demonstrated one or two orders of magnitude lower moduli due to absence of reinforcement, directly pinpointing the subtle effect of CNCs for the increased stiffness, while not sacrificing the high dynamics, as seen later. Strain-dependent oscillatory rheology demonstrated a broad linear viscoelastic regime up to strains of 10–20% (Figure 5b, S4 and S5). This deviation from linearity and subsequent decrease in both the oscillatory shear modulus and complex viscosity were observed on account of the selective breakdown of the dynamically cross-linked structure leading towards the easily flowing sol-state.

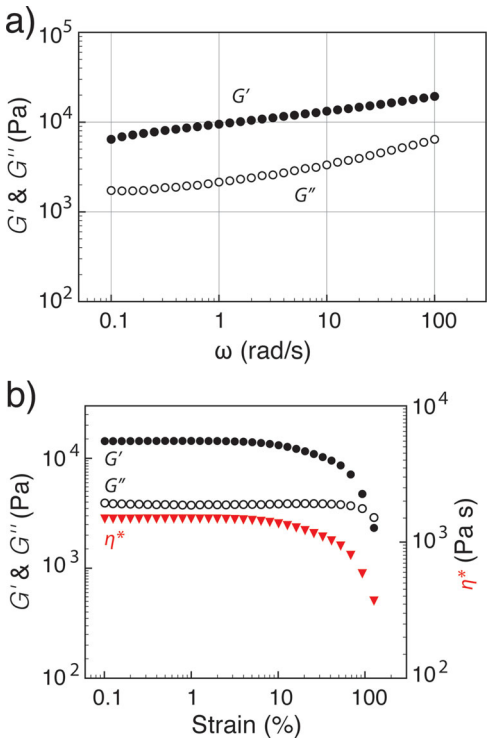

Figure 5. Rheology of CNC-*g*-P(DMAEMA-*r*-NpMA)/PVA-MV/CB[8] with Np and MV units at their molar ratio of 1.1, i.e. close to their stoichiometric binding in CB[8], (Table 1, entry 3). a) Frequency sweep shows that G' is essentially constant and $G' >> G''$ showing gelation. b) Strain-sweep with G', G'' and the complex viscosity η^*, collected at 10 rad/s.

2.5. Characterization by Electron Microscopy

The structure of the hydrogels was characterized by cryogenic transmission electron microscopy (cryo-TEM) and scanning electron microscopy (SEM). **Figure 6** shows a cryo-TEM micrograph for CNC-*g*-P(DMAEMA-*r*-NpMA)/PVA-MV/CB[8] with Np and MV units at their molar ratio of 1:1, showing that the rod-like CNC-*g*-P(DMAEMA-*r*-NpMA) species were homogeneously dispersed within the hydrogel without apparent aggregation. This was observed for all compositions (Figure S8). The SEM images revealed highly porous network structures for frozen and lyophilized samples (Figure S9).

2.6. Rapid Self-Healing and Temporal Stability

Step-strain rheological measurements of G' and G'' were then utilized to quantitatively investigate the re-forming kinetics of the aqueous networks by measuring alternatively at a low strain (0.05% for 120 s), immediately following the strain-induced gel-to-sol transition, measured at high strains (150% for 30 s) (**Figure 7** and S10). Figure 7c depicts the results for the stiffest hydrogel close to the stoichiometric composition

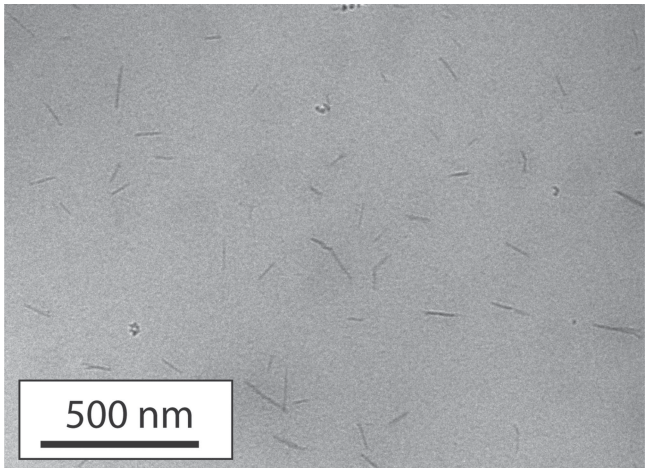

Figure 6. Cryo-TEM image of CNC-*g*-P(DMAEMA-*r*-NpMA)/PVA-MV/CB[8] with Np and MV units at their molar ratio of 1.1, i.e. close to their stoichiometric binding in CB[8]. The well dispersed CNCs are clearly resolved.

Np/MV = 1.1/1.0 mol/mol (Table 1: entry 3). A drop in *G'* of one order of magnitude upon rupture of the supramolecular cross-linking at high strains was observed. The non-stoichiometric and slightly weaker hydrogels displayed a larger two order magnitude drop in *G'* (Figure S10), likely on account of their lower solids content. It is striking that the materials, regardless of composition, completely recovered to their original *G'* and *G"* values within ca. 6 seconds, demonstrating no essential decay. These measurements further demonstrated that the rapid and reversible strain-induced rupture and re-formation of the dynamic cross-links occurred exclusively through cleavage of the CB[8] ternary complexes (Figure 7). To our knowledge, the time-range shown is the most rapid reported for hydrogels to date.

The particularly quick re-forming of the aqueous networks also manifested as fast healing of the hydrogel after macroscopic break. When the material was cut and the two pieces were immediately brought together even for a short time (30 s), the subsequent stretching qualitatively resulted in rupture at a different location along the material (**Figure 8**a). This indicates that the broken network was successfully re-formed. Figure 8b qualitatively demonstrates the fast healing of the material even after aging of the broken material for 4 months in a closed container at close to 100% relative humidity, a condition typically prohibitive for bare hydrogen bonded or ionically bound complexes systems.[1] Rapid self-healing was still observed after such prolonged aging due to the selectivity and dynamics allowed by the three-component recognition. This observation suggested that the specificity of the three-component recognition is a feasible route to solve the time-dependent passivation problem in self-healing hydrogels. The healing is therefore robust, rapid and does not require immediate repair – thus being in stark contrast to the previously reported supramolecular hydrogel systems.

These observations can be put in a more general context, where the engineering of the dynamics of reversible supramolecular or chemical bonds has recently allowed advanced materials properties. Supramolecular polymeric networks forming self-healing rubber-like networks in the solid-state have been described based on hydrogen bonds.[46] However, these 'bare' interactions were vulnerable against time dependent passivation phenomena due to formation of hydrogen bonds within the separated broken surfaces and moisture adsorption, thus inhibiting re-formation of the hydrogen bonding networks between the broken parts. More recently, catalyzed chemical exchange reactions have brought forth vitrimers.[47] These networks become malleable upon heating to high temperatures due to rapid exchange chemical reactions; while upon cooling, the materials freeze to the glassy state. Finally, dynamic and transient supramolecular bonds in combination with polymeric conformational degrees of freedom have yielded tough hydrogels as well as concepts for hydrogel glueing.[48,49] Therefore, the present concept shown herein with both high exchange dynamics and selectivity, combined with colloidal reinforcement may even pave ways towards new combinations of properties – such as combining increased hydrogel toughness based on sacrificial bonds and nanoscale reinforcement.

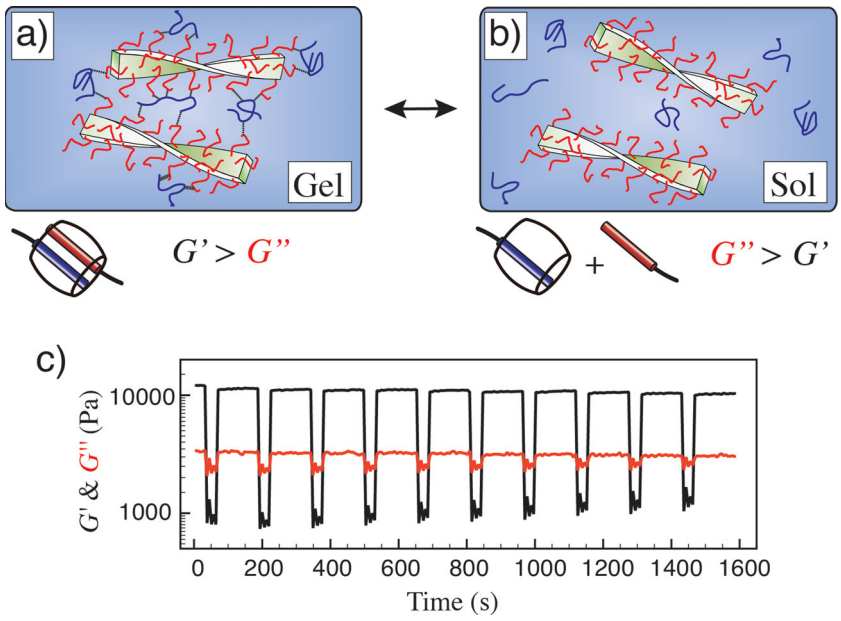

Figure 7. Rapid reversible sol-gel transitions as demonstrated by rheology for CNC-*g*-P(DMAEMA-*r*-NpMA)/PVA-MV/CB[8] with Np and MV units at their molar ratio of 1.1, i.e. close to their stoichiometric binding in CB[8] (Table 1, entry 3). a) Schematic representation of the hydrogel cross-linking on account of both naphthalene and viologen moieties binding inside CB[8] versus b) the sol-state whereby high strain results in dissociation of the ternary complex. The naphthalenes dissociate first. c) Periodic sol-gel transitions, upon application of low strains (0.05%, 120 s) and high strains (150%, 30 s).

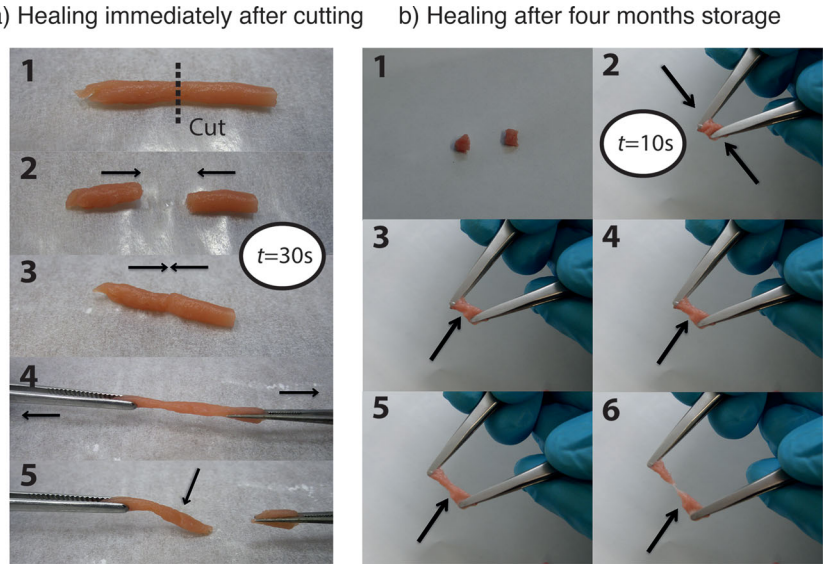

Figure 8. Qualitative demonstration of the self-healing of three-component recognition-driven hydrogel with a Np/MV molar ratio of 1.1 (Table 1, entry 3). a) Self-healing immediately after cutting. (1) Original hydrogel. (2) Cutting of the material followed by (3) self-healing by bringing the two cut pieces together for 30 s immediately after the cutting. (4) Subsequent stretching of the material resulted in (5) a new point of failure. b) Self-healing after 4 months of storage. (1–2) The pieces were brought together for 10 s via the exposed surface-area and stretched until break (3–6). The rupture was again observed at a different site.

3. Conclusions

By combining reinforcing 'hard' nanocrystalline cellulose domains with 'soft' supramolecularly cross-linked polymeric domains that utilized the highly dynamic and selective CB[8]-based ternary complexation capable of rapid exchange interactions, we have prepared hydrogels that synergistically combine three important yet seemingly conflicting criteria: rapid hydrogel recovery (on the timescale of a few seconds) from the processable sol-state; a high storage modulus; and suppressed passivation of self-healing as allowed by the specificity of the three-component recognition. The specific three-component recognition imparts rapid self-healing, even after ambient storage of the broken material over the course of several months, something that has not been previously demonstrated. This work suggests robust strategies to combine highly dynamic supramolecular interactions with mechanically strong colloidal reinforcements for the preparation of the next generation of advanced dynamic materials from renewable resources.

4. Experimental Section

Materials: All materials were purchased from Aldrich. DMAEMA monomer was purified by running it through basic alumina, and the cellulose nanocrystals, cucurbit[8]uril, and PVA-MV, were prepared according to literature procedures.[14,38] The other chemicals were used as received.

Synthesis of CNC-g-P(DMAEMA-r-NpMA) and PVA-MV: Br-modified CNCs used to initiate the surface-initiated atom transfer radical polymerization (SI-ATRP) were synthesized according to a protocol introduced previously.[38] SI-ATRP of DMAEMA 4905.0 mg, 31.2 mmol) and NpMA (933.0 mg, 3.12 mmol) was conducted in a CNC-Br (36 mg, n(Br) 0.016 mmol) suspension in DMF (3 mL) under an inert N_2 atmosphere. The reaction was catalysed with a Cu(I)/ hexamethyltriethylenetetramine (5.6 mg, 0.039 mmol and 18 mg, 0.078 mmol respectively) metal-ligand complex at 70 °C for 180 min. The colloidal product was purified via multiple centrifugation cycles (MeOH, DMF and 1,4-dioxane) and finally freeze-dried. Methylviologen functionalized PVA was synthesized according to previous studies.[14] More details are in Supporting Information.

Supporting Information

Supporting Information is available from the Wiley Online Library or from the author.

Acknowledgements

J. R. McKee and E. A. Appel contributed equally to this work. This work was partially funded by a European Research Council Starting Investigator Grant (ASPiRe) ERC-2009-StG-240629, an Engineering and Physical Sciences Research Council grant EP/F035535/1, and an ERC Advanced Grant Mimefun. O.I. and O.S. acknowledge ESF Precision Polymer Materials (P2M) network for initiation of this work. Aalto Nanomicroscopy Center is acknowledged for use of the devices. E.A. acknowledges Schlumberger for his PhD fellowship.

Received: October 31, 2013
Revised: December 29, 2013
Published online: March 4, 2014

[1] Q. Wang, J. L. Mynar, M. Yoshida, E. Lee, M. Lee, K. Okuro, K. Kinbara, T. Aida, *Nature* **2010**, *463*, 339.
[2] A. Harada, R. Kobayashi, Y. Takashima, A. Hashidzume, H. Yamaguchi, *Nature Chem.* **2011**, *3*, 34.
[3] M. Nakahata, Y. Takashima, H. Yamaguchi, A. Harada, *Nature Commun.* **2011**, *2*, 511.
[4] Y. Zheng, A. Hashidzume, Y. Takashima, H. Yamaguchi, A. Harada, *Nature Commun.* **2012**, *3*, 831.
[5] H. Yamaguchi, Y. Kobayashi, R. Kobayashi, Y. Takashima, A. Hashidzume, A. Harada, *Nature Commun.* **2012**, *3*, 603.
[6] Y. Takashima, Y. Yuting, M. Otsubo, H. Yamaguchi, A. Harada, *Beilstein J. Org. Chem.* **2012**, *8*, 1594.
[7] K. Haraguchi, K. Uyama, H. Tanimoto, *Macromol. Rapid Commun.* **2011**, *32*, 1253.
[8] A. Noro, M. Hayashi, Y. Matsushita, *Soft Matter* **2012**, *8*, 6416.
[9] A. Phadke, C. Zhang, B. Arman, C.-C. Hsu, R. A. Mashelkar, A. K. Lele, M. J. Tauber, G. Arya, S. Varghese, *Proc. Natl. Acad. Sci. USA* **2012**, *109*, 4383.
[10] P. H. J. Kouwer, M. Koepf, V. A. A. LeSage, M. Jaspers, A. M. van Buul, Z. H. Eksteen-Akeroyd, T. Woltinge, E. Schwartz, H. J. Kitto, R. Hoogenboom, S. J. Picken , R. J. M. Nolte, E. Mendes, A. E. Rowan, *Nature* **2013**, *493*, 651.
[11] E. A. Appel, J. del Barrio, X. J. Loh, O. A. Scherman, *Chem. Soc. Rev.* **2012**, *41*, 6195.
[12] G. L. Fiore, S. J. Rowan, C. Weder, *Chem. Soc. Rev.* **2013**, *42*, 7278.
[13] E. A. Appel, F. Biedermann, U. Rauwald, S. T. Jones, J. M. Zayed, O. A. Scherman, *J. Am. Chem. Soc.* **2010**, *132*, 14251.

[14] E. A. Appel, X. J. Loh, S. T. Jones, F. Biedermann, C. A. Dreiss, O. A. Scherman, *J. Am. Chem. Soc.* **2012**, *134*, 11767.
[15] N. Lin, A. Dufresne, *Biomacromolecules* **2013**, *14*, 871.
[16] J. A. Burdick, W. L. Murphy, *Nature Comm.* **2012**, *3*, 2271.
[17] The interplay between the cross-link dynamics and gel mechanical properties has been discussed, e.g., in D. H. Wachsstock, W. H. Schwarz, T. D. Pollard, *Biophys. J.* **1994**, *66*, 801. Note that in solid organic glass networks the possibility for interplay of rapid exchange interactions and high modulus has recently been pointed out, see ref. [47].
[18] J. Szejtli, *Chem. Rev.* **1998**, *98*, 1743.
[19] J. Kim, I.-S. Jung, S.-Y. Kim, E. Lee, J.-K. Kang, S. Sakamoto, K. Yamaguchi, K. Kim, *J. Am. Chem. Soc.* **2000**, *122*, 540.
[20] J. Lagona, P. Mukhopadhyay, S. Chakrabarti, L. Isaacs, *Angew. Chem., Int. Ed.* **2005**, *44*, 4844.
[21] K. Kim, N. Selvapalam, Y. H. Ko, K. M. Park, D. Kim, J. Kim, *Chem. Soc. Rev.* **2007**, *36*, 267.
[22] S. Kasera, F. Biedermann, J. J. Baumberg, O. A. Scherman, S. Mahajan, *Nano Lett.* **2012**, *12*, 5924.
[23] J. Zhang, R. J. Coulston, S. T. Jones, J. Geng, O. A. Scherman, C. Abell, *Science* **2012**, *335*, 690.
[24] J.-F. Revol, H. Bradford, J. Giasson, R. H. Marchessault, D. G. Gray, *Int. J. Biol. Macromol.* **1992**, *14*, 170.
[25] K. Fleming, D. G. Gray, S. Matthews, *Chem. Eur. J.* **2001**, *7*, 1831.
[26] Y. Habibi, L. A. Lucia, O. J. Rojas, *Chem. Rev.* **2010**, *110*, 3479.
[27] S. J. Eichhorn, *Soft Matter* **2011**, *7*, 303.
[28] G. Siqueira, J. Bras, A. Dufresne, *Polymers* **2010**, *2*, 728.
[29] J. R. Capadona, O. van den Berg, L. A. Capadona, M. Schroeter, S. J. Rowan, D. J. Tyler, C. Weder, *Nat. Nanotechnol.* **2007**, *2*, 765.
[30] K. E. Shopsowitz, H. Qi, W. Y. Hamad, M. J. MacLachlan, *Nature* **2010**, *468*, 422.
[31] M. V. Biyani, E. J. Foster, C. Weder, *ACS Macro Lett.* **2013**, *2*, 236.
[32] T. Saito, S. Kimura, Y. Nishiyama, A. Isogai, *Biomacromolecules* **2007**, *8*, 2485.
[33] T. Saito, R. Kuramae, J. Wohlert, L. A. Berglund, A. Isogai, *Biomacromolecules* **2013**, *14*, 248.
[34] Q. Xu, J. Yi, X. Zhang, H. Zhang, *Eur. Polym. J.* **2008**, *44*, 2830.
[35] G. Morandi, L. Heath, W. Thielemans, *Langmuir* **2009**, *25*, 8280.
[36] G. Morandi, W. Thielemans, *Polym. Chem.* **2012**, *3*, 1402.
[37] J. O. Zoppe, Y. Habibi, O. J. Rojas, R. A. Venditti, L.-S. Johansson, K. Efimenko, M. Österberg, J. Laine, *Biomacromolecules* **2010**, *11*, 2683.
[38] J. Majoinen, A. Walther, J. R. McKee, E. Kontturi, V. Aseyev, J.-M. Malho, J. Ruokolainen, O. Ikkala, *Biomacromolecules* **2011**, *12*, 2997.
[39] F. Biedermann, O. A. Scherman, *J. Phys. Chem. B* **2012**, *116*, 2842.
[40] Y. Zhang, Z. Yang, F. Yuan, H. Gu, P. Gao, B. Xu, *J. Am. Chem. Soc.* **2004**, *126*, 15028.
[41] L. E. Buerkle, H. A. von Recum, S. J. Rowan, *Chem. Sci.* **2012**, *3* 564.
[42] J. N. Hunt, K. E. Feldman, N. A. Lynd, J. Deek, L. M. Campos, J. M. Spruell, B. M. Hernandez, E. J. Kramer, C. J. Hawker, *Adv. Mater.* **2011**, *23*, 2327.
[43] F. Peng, G. Li, X. Liu, S. Wu, Z. Tong, *J. Am. Chem. Soc.* **2008**, *130*, 16166.
[44] W. Burchard, S. B. Ross-Murphy, Physical Networks; Polymers and GelsElsevier, London, UK **1990**.
[45] K. te Nijenhuis, Thermoreversible Networks; Viscoelastic Properties and Structure of GelsSpringer-Verlag, Berlin, Germany **1997**.
[46] P. Cordier, F. Tournilhac, C. Soulie-Ziakovic, L. Leibler, *Nature* **2008**, *451*, 977.
[47] D. Montarnal, M. Capelot, F. Tournilhac, L. Leibler, *Science* **2011**, *334*, 965.
[48] K. Mayumi, A. Marcellan, G. Ducouret, C. Creton, T. Narita, *ACS Macro Lett.* **2013**, *2*, 1065.
[49] S. Rose, A. Prevoteau, P. Elzière, D. Hourdet, A. Marcellan, L. Leibler, *Nature* **2013**, *505*, 382.